J Ther Eng, Vol. 10, No. 5, pp. 1164−1183, September, 2024

Journal of Thermal Engineering
Web page info: https://jten.yildiz.edu.tr
DOI: 10.14744/thermal.0000859

Research Article

Energy, exergy and performance analysis of a 380 kW_P roof-top PV plant assisted with data-driven models for energy generation

Abhijeet RATHORE[1], ALMAS[1], Sivasankari SUNDARAM[1,*]

[1]*Energy Institute Bengaluru, Centre of RGIPT, Bengaluru, 562 157, India*

ARTICLE INFO

Article history
Received: 26 December 2022
Revised: 15 May 2023
Accepted: 22 May 2023

Keywords:
Deep-learning and 380 kW_p PV Plant; Energy Efficiency; Exergy Efficiency; Testing for Non-trained Location

ABSTRACT

Energy and Exergy based performetric analysis integrated with deep learning assisted energy modelling for grid connected solar PV system, tested to non-trained location is proposed. The first objective is to perform an energy and exergy based performetric analysis for a realistic 380 kW_p grid connected roof-top PV system whose performance parameter is used for testing the proposed energy prediction models. The second objective is to formulate a simple and an improved energy estimation method applicable for 34 locations in South India, without change in model-coefficients. So, a long-term annual performance analysis of a 380 kW_p PV based distributed generator situated at 12.97°N and 77.59°E is performed which estimates the characteristic performance indicators like energy efficiency, exergy efficiency, performance ratio and capacity factor amounting to 8.49%, 1.03%, 37%, and 8.03% respectively. The performance ratio of the plant is less as evident from the least exergy efficiency. The annual average losses in the system like thermal capture loss, array capture loss, system loss and miscellaneous loss amount to 0.46 (h/d), 2.51(h/d), 0.71 (h/d) and 2.97(h/d) respectively. The annual average energy generation of 380 kW_p is 732.84 kWh/year. Furthermore, for realizing the second objective, a total of four models are proposed namely linear, exponential, non-linear and deep learning based neural network model resulting in R of 0.933, 0.9071, 0.9386, and 0.9603 respectively is formulated. The proposed models are tested for non-trained locations where the R value justifying the closeness between the actual and the predicted value is as high as 0.8. The proposed models are then compared upon their performances and benchmarked against the reported models.

Cite this article as: Rathore A, Almas, Sundaram S. Energy, exergy and performance analysis of a 380 kW_P roof-top PV plant assisted with data-driven models for energy generation. J Ther Eng 2024;10(5):1164−1183.

INTRODUCTION

In recent years, several factors have led to enhanced inception of renewable energy in the conventional grid system which includes, global warming, carbon emissions, exhaustion of fossil fuels, soaring conventional fuel price, and concerns about rising environmental equivalent potentials. As per the reports of International Energy Agency

***Corresponding author.**
*E-mail address: sivasankari66@gmail.com; ssundaram@rgipt.ac.in

This paper was recommended for publication in revised form by Editor-in-Chief Ahmet Selim Dalkılıç

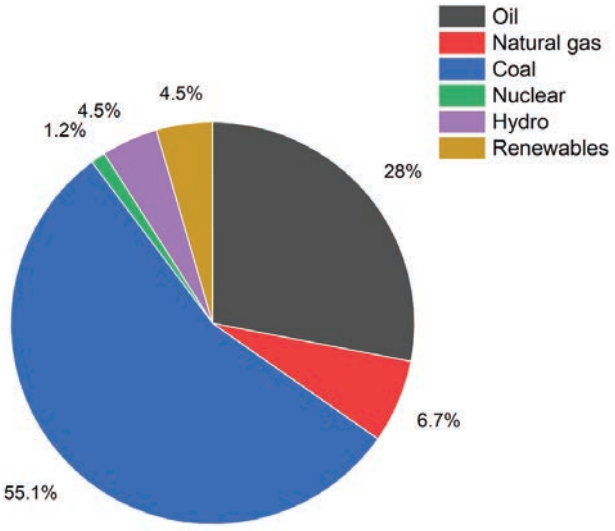

Figure 1. Global share of primary consumption of different energy resources.

(IEA), fossil fuels (coal, natural gas and oil) still prevail to be a major resource of primary energy generation across the globe and occupying 89.8% of the installed capacity especially in India, as indicated in Figure 1 [1].

Hydropower and renewable also contributed equally to the installed electricity capacity amounting to 4.5%. In the year 2020, the overall primary energy consumption for India was 31.98 EJ out of which the share of renewable energy was 1.43 EJ [2]. The increase in renewable installations contribute to the energy mix thereby delivering improved sustainability index and preserve primary energy resources. If the usage of coal, oil and natural gas are left unmonitored, this shall lead to economic as well as political conflicts of great magnitude [3,4]. Renewable energy resources are present in surplus quantity in nature and thus can be easily harnessed to extract the required energy. Even a small percentage of the available solar energy can meet the current demand all over the globe [5]. Among all other technologies, solar energy is gaining more momentum these days [3-6]. In the year 2018, Solar energy comprised 55% of total renewable energy installations-based enhancement followed by Wind and Hydro. Among installed renewable energy capacity, Solar power installation occupies a larger occupant area of around 53%, in comparison with other renewable energy installations as seen in Figure 2 [CEA document]. Bio-energy also occupies a quantifiable fraction of 8.4% towards energy installations.

In accordance with the Statistical review of world energy, 2021 [2], there has been the largest ever increase in renewable energy generation i.e., 358 TWh and there is the largest-ever drop in oil production across the globe i.e., -6.6 Mb/day. There is also the largest ever rise in the share of solar in non-conventional energy generation. The share of renewable energy has increased in recent years as opposed to the reduction in shares of conventional energy resources such as oil and nuclear energy as evident from Figure 1. Solar has a global contribution of 148 TWh. Solar energy is developing as an important alternative to primary energy, as it has the property of easier collection, conversion, and usage. Solar PV installations are an excellent source of decentralized power units even in places where the installation of conventional electric grid becomes difficult. It is made utilizable on creation of integrated system with the grid. This improved deployment of renewable generating systems has led to a growth in its related research and their integration with the grid.

PV Installation though possess benefits on usage, its stochastic nature creates certain complexities in the

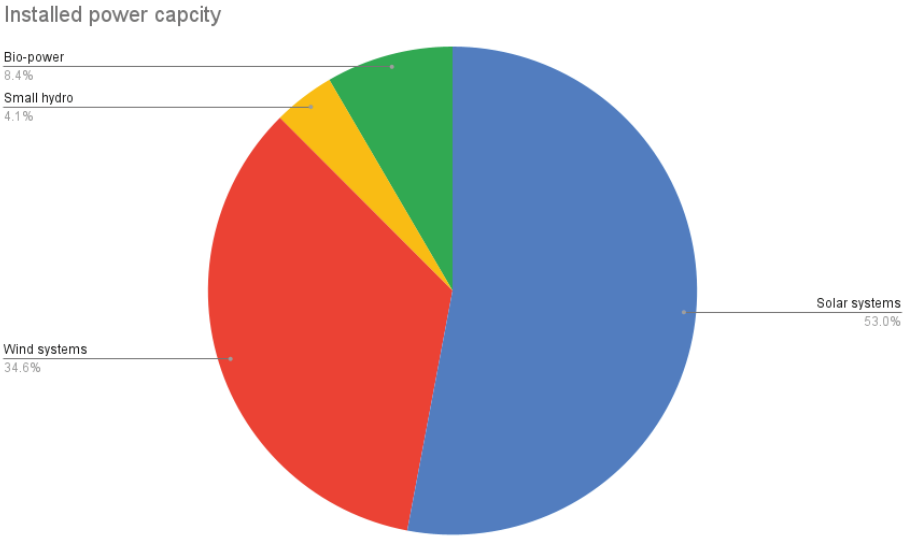

Figure 2. Installed capacity of solar and wind power in India.

Table 1. Major Limitations of the reported investigations

S. No	Major Limitations of the reported energy prediction models
1	The reported models as discussed were majorly formulated and validated only for a single location.
2	The trained location for model formulation and tested location for model validation were the same.
3	Consideration of truly significant factors affecting desired response (energy generation) remains majorly unreported

aspects of power distribution. These include power quality disturbances, supply-demand balance, load scheduling and generation scheduling impacting grid system operators to ensure reliability [7]. As the present revamped electric grid encompassing DES (distributed energy sources) is not a constant producer-controlled network, the grid operators should ensure a tenacious balance of supply and demand. Furthermore, a solar design Engineer must practically ensure the technical feasibility of a solar power plant before installation [8]. These deliverables can be achieved only when the knowledge on energy yield is priorly and accurately known by the system operator / control centre for controlling the grid [9-11]. So, a tool for accurate estimation of power output for a distributed energy network will enable reliability of power supply and creates convenience for the grid operator to optimally schedule the operating system. Therefore, the review of literature as cited below involves mathematical tools applicable for estimation of energy/ power generated by a Solar PV system on-field.

Recent research on formulation and development of predictive and accurate energy prediction models were reported by a few researchers as examined below. Huang et al. [12] proposed a short-term day ahead forecasting model for PV power prediction using a Convolutional Artificial neural network (CNN) based approach. The features considered encompass historical PV power, direct normal irradiance, ambient temperature and ambient humidity. Meng et al. [13] analysed extreme-short-term forecasting for PV power under clouded/ shaded conditions using neural network approach. The model also encompassed the speed and direction of the moving cloud, to depict the PV power. Yan et al. [14] attempted extreme-short-term forecasting model for estimating the power produced. A frequency domain-decomposition-based neural network model was formulated for trained locations. The study enabled prediction of the response variable 15 minutes ahead. Ahmed et al. [15] reviewed many past works of literature which provided significant update of forecasting techniques for solar PV power prediction and compared them based on the value of RMSE as well as forecasting horizon. Out of all the considered techniques, ANN and CNN proves to be more accurate in terms of forecast accuracy, especially for short-term forecast [16-19]. In addition, case studies of harnessing Solar energy are depicted by Bhowmik et al. [17,18]. Kim et al. [20] formulated a model based on regression approach after successful identification of significant factors affecting the PV power output, for the location of Korea. Statistical error comparison for the reported models was also discussed. Sheng et al. [21] formulated a forecasting model for Solar PV output using a weighted gaussian regression model for a training location of Nanyang Technological University Singapore. Smithsonet al. [22] also justified the importance of employing neural network-based approach for intermittently varying system inputs. The major limitations of the reported investigations are précised in Table 1.

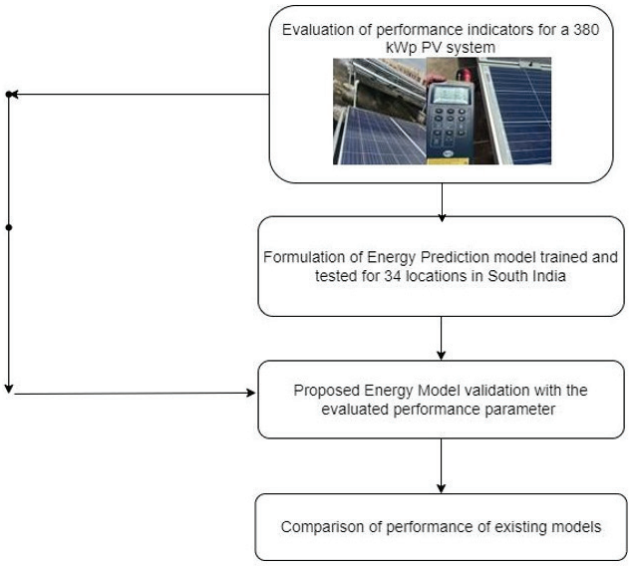

Figure 3. Stages of investigation.

These limitations resulted in the present objective involving development of a robust and generalized model which estimates the long-term monthly average daily value of energy generation by a PV system. The tool is formulated for 34 locations of South India coupled with realistic system-based performance analysis. The locations considered for training and testing are entirely different, covering major of south Indian locations. The presented research investigation is carried out in two different stages as seen in Figure 3. The first stage is on on-field performance investigation of the distributed PV plant and the other is on formulation of accurate energy prediction model. The detailed specifications of equipment employed are provided in Table 2.

Table 2. Specification of the instruments used in experiment

S.No	Name of instrument	Open circuit voltage Voc	Short circuit current Isc	Operating Current	DC Power	Irradiance	Temperature	Compass Bearing	Inclinometer
1	I-V Curve Tracer	1000V DC	15A DC	40A	40kW	-	-	-	
2	Solar Survey(200R)	-	-	-	-	100-1250 W/m^2	-30^o C to +125^0 C	0^0 to 90^0	0^0 to 90^0
3	PV module Temperature	-	-	4-20 mA	-	-	0 to 100^o C	-	-

PERFORMETRIC ANALYSIS

In order to determine the operational characteristics for PV system over a long-term perspective in an area, performance assessment should be carried out inevitably. The evaluated performance indicators are employed as testing data for formulation of energy prediction model/ design tool. The total losses that occur in the plant are also quantified with the help of detailed performance analysis. Furthermore, exhaustive technical analysis provides information on the annual operational characteristics of distributed PV system on a monthly average daily basis. The information obtained helps the policy makers, interested individuals and organization to understand and compare the actual performance of PV system as the installed locality. This analysis is traditionally carried out by measuring and monitoring the actual AC and DC energy output of the PV plants. These dynamically measured variables are employed for estimation of performance indicators as described in IEC standard 611724 [23]. The evaluated parameters are employed as training/ testing data set for our proposed energy model formulation. Figure 4 describes the single line diagram of a roof-top grid connected 380 kW_p PV plant situated with co-ordinates of 12.97^{0}N and 77.59^{0}E. The system under consideration encompasses a 380 kWp grid connected PV system located inside NITTE Meenakshi Institute of Technology Bengaluru the capital of Karnataka, India.

The modules were Poly-crystalline manufactured by GERMAN SOLAR. The total number of PV modules installed were 1170 with each having a rating of 325 W_p equally contributing to a total rating of 380.2 kW_p. There are 6 inverters each having a capacity of 60 kW. Each string comprised of 18 panels and 11 strings were connected to a single inverter. The orientation of the panels was permanently facing south with a tilt angle of 13°.

An exhaustive performance analysis is carried out annually for duration of the measured inputs between January 2021 to December 2021 with evaluation of characteristic

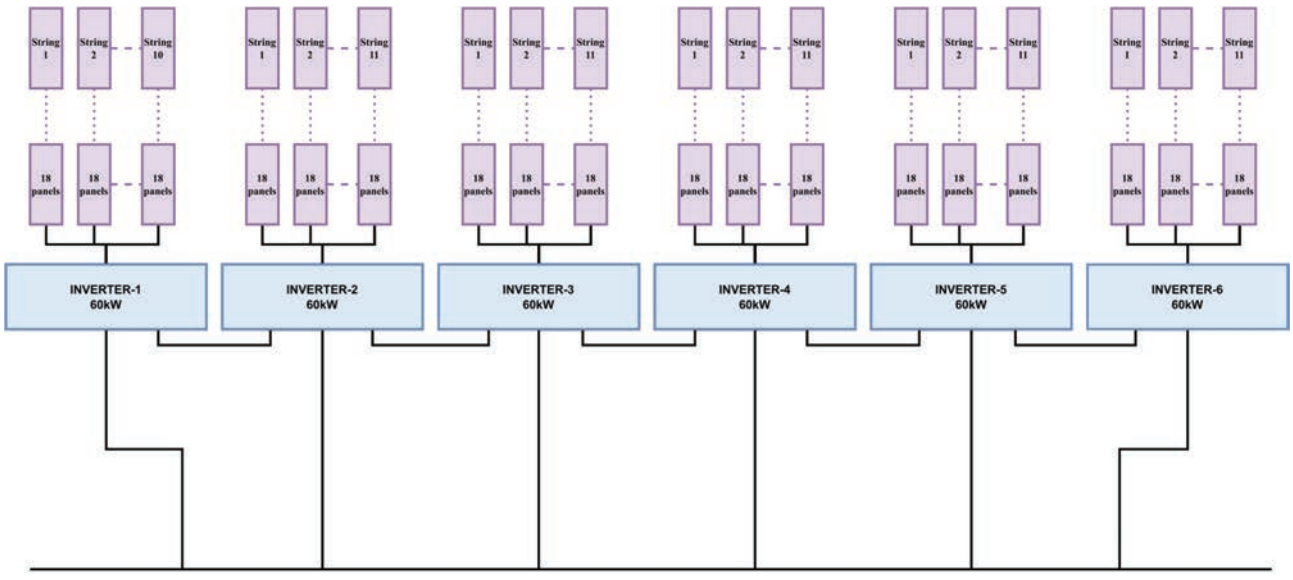

Figure 4. Single line diagram of 380 kWp PV array installed at NMIT, Bangalore with 1170 panels.

Figure 5. PV200 I-V curve tracer.

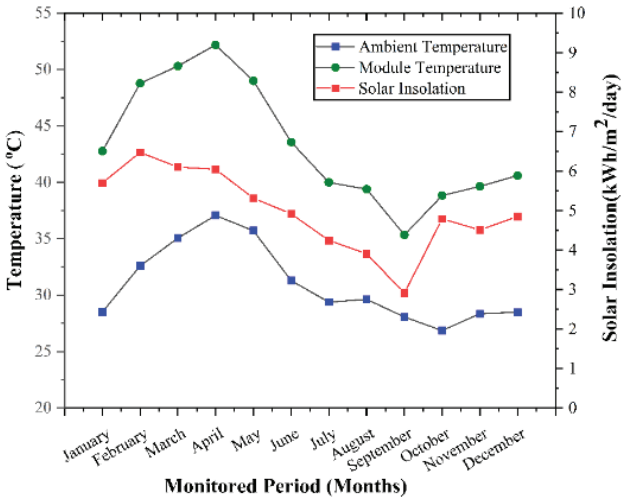

Figure 6. Solar insolation, PV module and ambient temperature for the monitored period.

indicators like final yield (Y_F), capacity factor (CF) and performance ratio (PR) [23]. These parameters act as comparators among other PV systems which states the operating index of the plant.

The measured input parameters for the location are global horizontal irradiance at tilt, PV module and ambient temperature. These are measured employing an Irradiance meter, Pt 100 temperature sensor and back surface vacuum-based temperature sensor which comes integrated to PV200 Solar I-Vcurve analyser as shown in Figure 5. The measured inputs showing the annual variation of irradiance, ambient temperature and module temperature for the monitored duration is illustrated in Figure 6.

As seen from Figure 6, the average ambient temperature for the monitored period January 2021 to December 2021 is 28.10°C. The value of the module temperature is observed to be higher than the ambient as heat energy is generated with simultaneous generation of electrical power output, due to photovoltaic effect. The average module temperature for the monitored period is 43.4°C. The module temperature is higher during the period of March 2021 to June 2021 as the solar insolation is correspondingly higher for these periods ranging from 2.9 kWh/m²/day to 6.4 kWh/m²/day.

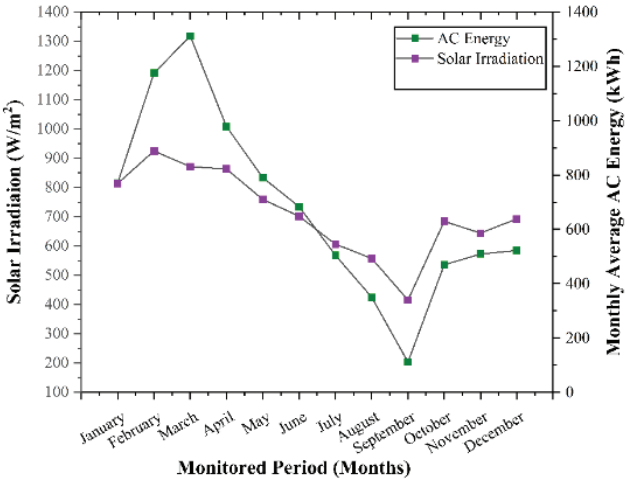

Figure 7. AC energy generated and solar insolation for the monitored period.

AC Energy Output (Eac)

The A.C energy generated by the PV system is measured across the inverter end at instants of recording time interval. The data is recorded for every 10 minutes. The daily and monthly net energy generated by the PV systems are obtained as [24]:

$$E_{AC,d} = \sum_{t=1}^{R_{tp}} V_{AC} * I_{AC} * R_T \; ; E_{AC,m} = \sum_{d=1}^{N_p} E_{AC,d} \quad (1)$$

R_T represents the meter recording time interval and R_{tp} is the reporting duration; N_p is the total operating days of the system in a month. V_{ac} and I_{ac} represent the voltage and resulted current appearing across inverter.

As seen from Figure 7, the monthly average energy generated by the PV system at the inverter end, is at its maximum in the month of March 2021 i.e. 1317.9438 kWh/month. The energy generation measured across the inverter varies synchronously with the irradiation incident on-field. The output AC energy is also affected by factors like average module temperature, tilt angle and orientation, manufacturing tolerance of modules and effect of accumulated dirt on modules.

Array Yield (Ya)

As per IEC 61724, array yield represents the operational hours of the PV module per day to produce DC energy equivalent to its rated output power. It is expressed as

$$Y_A = \frac{E_{A.DC}}{E_0} \ (h/d) \quad (2)$$

where $E_{A.DC}$ is the total energy output of PV array and E_o is installed watt peak capacity. The array yield for the 380 kW_p PV plant under consideration is 2.64 h/day whose variation is as seen in Figure 8. The array yield is higher for the period of February and March. This is due to the fact that the average irradiance is high as 925 W/m² during February and March in comparison to other months. Similarly, the array yield is lower for the months of August to December since the corresponding average irradiance is low as 415.37 W/m².

Reference Yield (Yr)

Reference yield represents the maximum potential available at a particular location. It is provided by the ratio of in-plane irradiance (H_T) to the standard test conditions of irradiance [25]. The reference yield provides a value normalized to the value of irradiance corrected to standard test conditions. For the current study Y_r ranges from an average of 4.8 to 6.4 h/d whose monthly average variation is expressed in Figure 8.

$$Y_R = \frac{H_T}{G_O} \text{ (h/d) or } kWh/kW_p \quad (3)$$

Final Yield (Yf)

The net energy output (E_{AC}) observed daily, monthly, or annually of the PV plant per watt peak of installed output power (E_0) at standard test conditions is denoted as final yield [25].

$$Y_F = \frac{E_{AC}}{E_o} \ kWh/kW_p \text{ or (h/d)} \quad (4)$$

The final yield for the 380 kWp PV plant under consideration is 1.92 h/d as represented in Figure 8. As there exist a linear correlation between array yield and final yield, the final yield is also found higher for the period of February and March and lower for the months of August to December.

Performance Ratio (PR)

Performance ratio has no dimension as it quantifies the total losses in the system. PR is a critical parameter, which is used to assess the operational quality. It acts as a unique performance comparator irrespective of the watt peak capacity of the power plant. This comparator plays a major role in ranking the operational characteristics of the system. Higher the PR good is the operation of the PV plant. The performance ratio provides an idea on the total losses that occur in the plant. The losses in the plant can be attributed to tripping of circuit breaker, failures due to solder-bonds in junction boxes, snow, soiling, shading, diode failures, failure in inverter operation, degradation of PV systems etc. It is given expressed as a ratio of Y_f to Y_r. The reported value of PR for Indian Conditions varies from 0.6 to 0.9 [26, 27].

$$PR(\%) = \frac{Y_F}{Y_R} \quad (5)$$

The closer the value to unity, the best is the operational performance of the plant. For the current investigation, the PR ranges from 0.37 to 0.56 as shown in Figure 9. This indicates that there occurs major power loss due to degradation-based aspects which shall form the scope for future work.

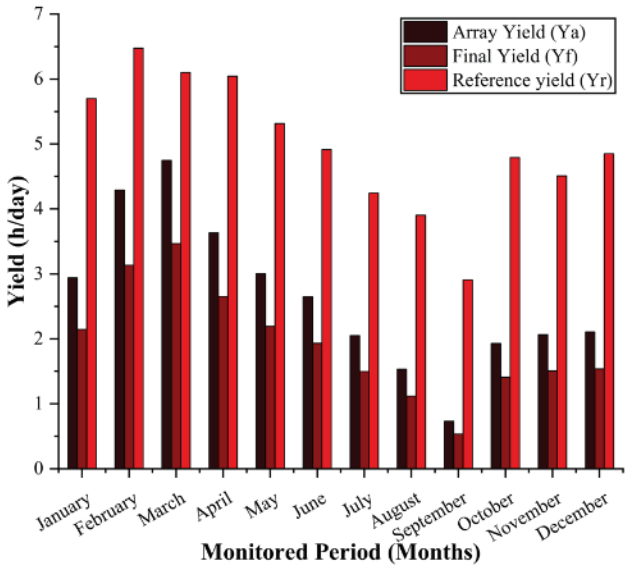

Figure 8. Evaluated reference yield (Y_r), final yield (Y_f) and array yield (Y_a) for the monitored period.

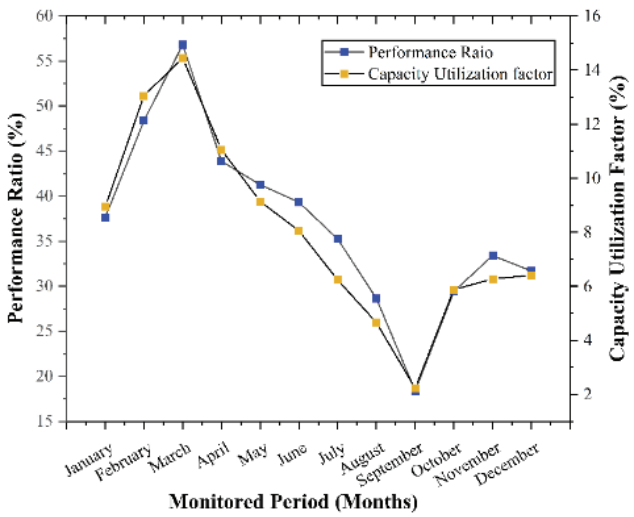

Figure 9. Performance ratio, capacity utilization factor vs. monitored period.

Capacity Utilization Factor (CUF)

CUF depends on the effective operational time period of the PV plant. It also depends on other location-based parameters like plane of array irradiance and total number of sunny days. It signifies the usage factor of the PV plant to generate the required AC power output. It is expressed in% and is given by

$$CUF(\%) = \frac{Y_F}{24 * 365} = \frac{E_{AC}}{E_0 * 24 * 365} * 100 \quad (6)$$

For the current analysis, the capacity utilization factor is 8.03%, as seen in Figure 9. CUF is at its peak in the month of February which varies in accordance with the PR.

Losses and Efficiency

The occurrence of energy losses in a PV system can be attributed to inherent changes experienced in the meteorological parameters and component-based degradation loss factors that occur in the system. Under on-field conditions the following losses affect the performance of a PV system.

- Thermal losses occur due to higher module temperature.
- Optical reflection loss and losses attributed to shadowing effects.
- Intermittent inverter operation intermittency at the inverter end.

The monthly average array loss, thermal capture loss, miscellaneous loss and system loss depend upon the array yield, final yield and the operating temperature. This is quantified for the system under investigation as represented in Figure 10. The average thermal capture loss, miscellaneous ca loss and system loss amounts to 0.46 (h/day), 2.97 (h/day) & 0.71 (h/day). Figure 11 presents the evaluated PV module efficiency and system efficiency during the monitored period. System efficiency depends on the operational efficiency of all the components. It is the

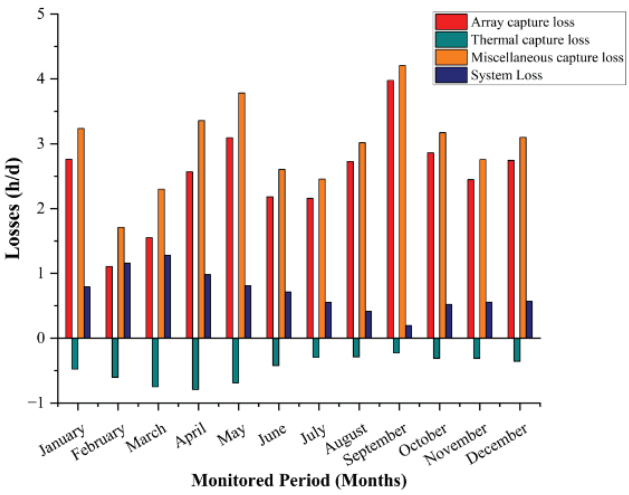

Figure 10. Monthly average losses for the monitored period.

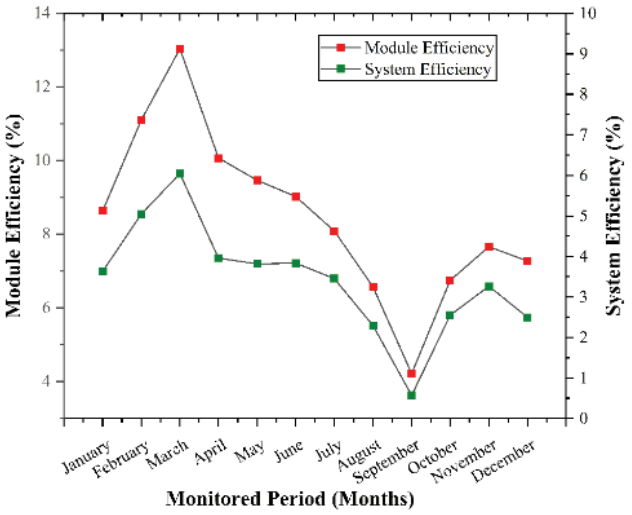

Figure 11. Module efficiency and system efficiency vs. monitored period.

product of PV module efficiency and inverter efficiency computed on the evaluated time horizon. However, the PV module efficiency depends on the in-plane solar irradiance and the energy generation. The system efficiency is better when the module performs better. As seen from Figure 11, system efficiency is at its minimum (2%) in the month of September as the solar radiation is only about 4.71(kWh/m^2/day). The system efficiency varies from 2% to 10%. The system efficiency is considerably higher for the month of March to May, where the solar insolation is higher. The performance of an operating PV system is also affected by losses due to convection and radiation modes in power generation of a PV cell.

Exergy Efficiency of the PV System

Exergy Efficiency of a distributed generator is derived from the second law of thermodynamics and is quantified as the ratio of output exergy to input system exergy [28].

$$\eta_{ex} = \frac{Exout}{Exin}; \text{ where }, \quad (7)$$

$$Ex_{(out)} = P_{pv} - \left(1 - \left(\frac{T_a}{T_m}\right)\right)[5.7 + 3.8 * v) * A * (T_m - T_a)]$$

T_s represents the sun's temperature; v is wind speed (m/s); A represents the area of the PV module; H is the irradiance; P_{pv} is the instantaneous power output generated by PV system and T_a and T_m represent the ambient and module temperature respectively.

$$Ex_{(in)} = \left(\left(1 - \left(\frac{4}{3} * \frac{T_a}{T_s}\right) * H * A\right)\right) \quad (8)$$

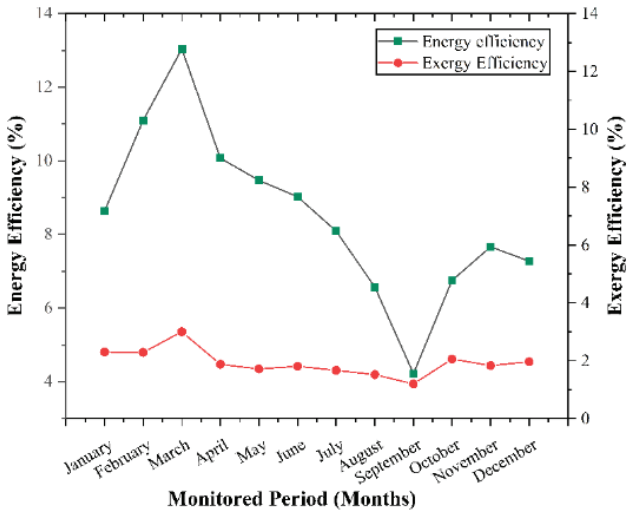

Figure 12. Monthly average energy and exergy efficiency.

The estimated annual average value of energy and exergy efficiency of the 380kW$_p$ system quantifies to 8.49% and 1.83% respectively as shown in Figure 12. The energy efficiency is relatively higher for the period of summer quantifying to an average of 8.94% in comparison to 6.91% in winter. This occurs due to the impact of global solar irradiance measuring 755W/m^2 for the duration of summer than 650 W/m^2 for the winter season. The thermal energy destruction encompassing thermal capture and array capture loss is 0.46 (h/day) & 2.51 (h/day) which causes reduction in the exergy efficiency than energy efficiency.

Table 3 shows a comparative analysis of the presented investigation with previous reported literature pertaining to the performance analysis of solar photovoltaic system. It is evident from the comparison that the 380 kW$_p$ PV system has more power loss attributed due to environmental conditions and degradation failures making the average value of performance ratio to be as less 0.3.

Model Formulation

The energy modelling process begins with consideration of location-based inputs influencing the energy output of the Solar PV system. Initially, factors pertaining to a location as indicated in Table 4 were considered for the model formulation. The developed model acts as an objective function consisting of decision variables as indicated in Table 4, for estimating the energy generation of a realistic Solar PV plant. However, re-formulation of the proposed model was attempted towards accurate results. The proposed model considers only the significant inputs which affect the predicted response. The dependence between the input and output is statistically realized through the p-value. The computed p-value is as shown in Table 4. Generally, the p-value should be below 0.05, which represents a significance of 95% for the selection of the considered input.

As inferred from Table 4, the variables with a p-value of less than 0.05 are Incident irradiance (H), ambient temperature (T_a), and Windspeed (w). This reveals that they contribute significantly to energy estimation and thus are included for the improved model formulation.

The training data is acquired from RETSCREEN software by National Renewable Energy Laboratory (NREL). A total of 10 locations in Southern India were designated for

Table 3. Comparative analysis of current work with previous literature

S.No	Plant Location only in India	Plant Capacity	PR%	CUF%	Reference number
1	Sivagangai, Tamil Nadu	5 MW$_p$	89.15	22.9	[23]
2	Lucknow, Uttar Pradesh	5 kW$_p$	76.97	16.39	[24]
3	Kaveripallayam, Tamil Nadu	1 MW$_p$	40	____	[29]
4	Ramagundam, Andhra Pradesh	10 MW$_p$	86.12	17.68	[30]
5	Karnataka	3 MW$_p$	78	15	[31]
6	Bengaluru, Karnataka	380 kW$_p$	37	8.03	Present study

Table 4. Selection of input parameters based on p-value

Input parameter	p-value
Global Horizontal Irradiance (GHI)	1.5784x10^{-5}
Ambient temperature	0.0386
Precipitation	0.9512
Pressure	0.5789
Windspeed	0.0273
Earth temperature	0.2904

Table 5. Forms of proposed models

Type of Model	Name
Linear Model	Model-1
Exponential Model	Model-2
Non-linear Model	Model-3
ANN	Model-4

formulation of the proposed model. They are Bengaluru, Coimbatore, Hyderabad, Calicut, Thiruvananthapuram, Tiruchirappalli, Anantapur, Sholapur, Ratnagiri, and Pune. The locations are selected based on the availability of ground-based solar radiation resource assessment (SRRA) stations. As the model is formulated from SRRA, it is believed to be accurate and adaptable to several other ground-based locations majorly covering regions of South India. The present research investigation proposes four independent models and provides an exhaustive comparison among them. Table 5 shows the terminology of the proposed models used in this paper.

Before approaching model formulation, it is important to normalize the training dataset such that it becomes independent of its standard international units. Generalization of model co-efficient cannot be made if the training data set is not normalized.

A multiple–linear regression model is firstly proposed incorporating statistically significant inputs like global horizontal irradiance, ambient temperature, and wind speed as shown in equation (9), typically applicable for South Indian Locations. The training of data or model formulation was performed in MATLAB employing error minimization approach. The R-value during training was found to be 0.933 with a root mean square error of 0.0751 and mean absolute error of 0.0602. The comparison of the actual and the formulated model for all the training locations is shown in Figure 13. The linear model formulated is given in equation (9). As observed from Figure 13, there lies a discrepancy between the estimated and the actual /observed values, which resulted in the formulation of subsequent models described as follows.

$$\boldsymbol{E = 0.1974 + 1.1395(H) - 0.4138(T_m) - 0.1988(w)} \quad (9)$$

The second model (Model -2) is the exponential model as shown in equation (10). It yields an R value of 0.9071 at the time of training but gives better performance in the case of test and validation. The RMSE of this model is 0.0873 with mean absolute error of 0.0710. The comparison between actual and predicted values is given in Figure 14. As seen in the figure, the closeness between the observed and the modelled value improves.

$$E = e^{2.1319(H) - 0.85(T_m) - 0.47(w) - 1.2579} \quad (10)$$

The third design tool is a non-linear model proposed for energy prediction, named model-3. The value of R with training data set is 0.9386 rendering an RMSE of 0.2143 and MAE of 0.1782. The formulated model function is given in equation (11). It gives by far the best performance among the previously formulated models as in equations (9) and (10). The same is reflected in Figure 15.

$$E = \frac{H}{0.5365 - 0.052(H) + 0.661(T_m) + 0.4731(w)} \quad (11)$$

An additional model based on deep-learning neural network-based structure has been formulated in MATLAB as shown in Figure 16. A neural network is a powerful tool for the prediction of time-series response which is dynamic in nature. The input variables for the proposed model as suggested from p-value analysis are global irradiance, module temperature and wind speed at the time instant 't'. These act as inputs for estimating the energy generated at the

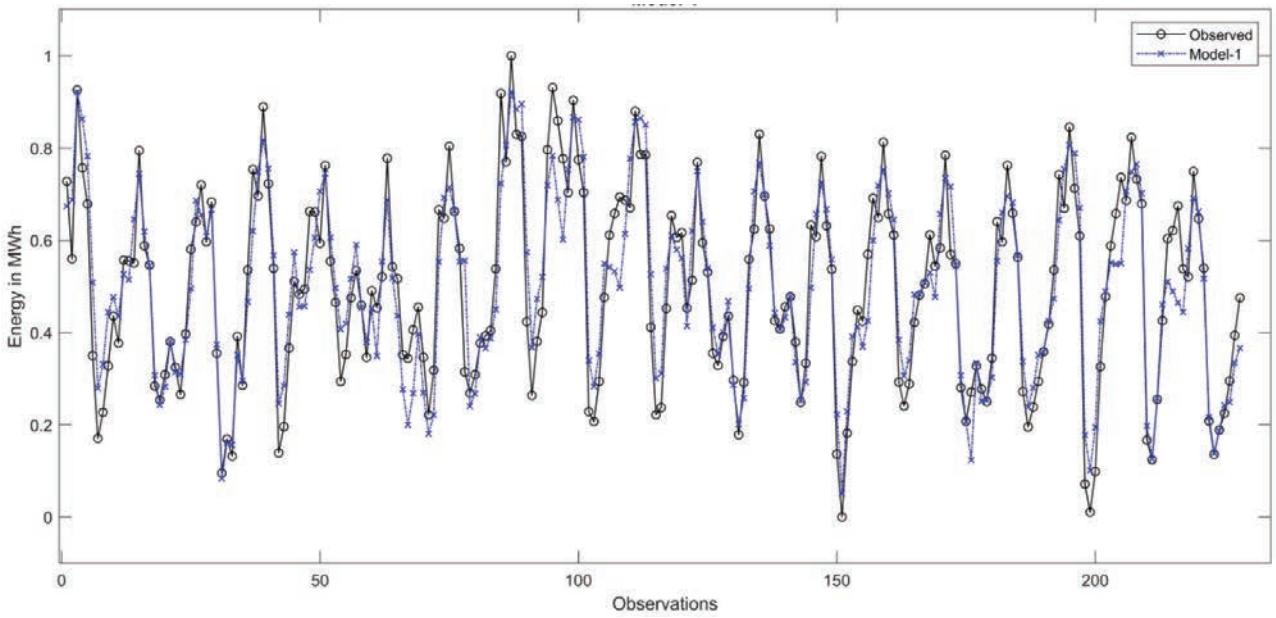

Figure 13. Comparison of actual vs. predicted values of energy for the linear model.

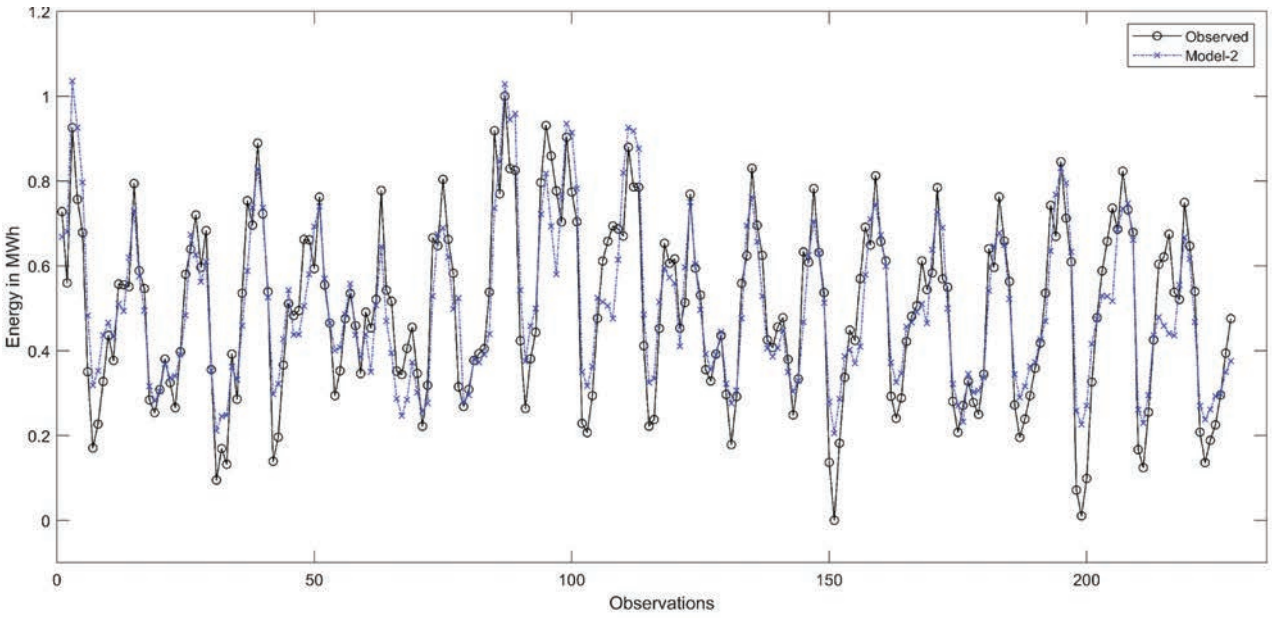

Figure 14. Comparison of actual and predicted values for the exponential model.

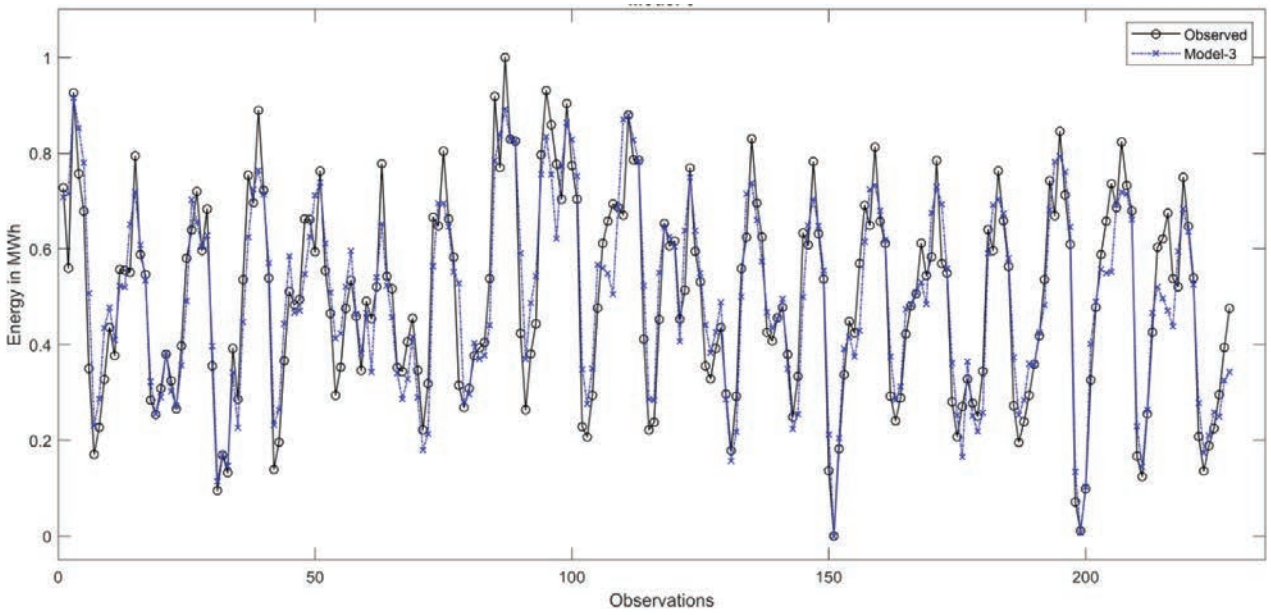

Figure 15. Calculated vs. actual model comparison for the non-linear model.

corresponding time. This behavior is truly adopted to neural network-based algorithms than machine learning algorithms whose function is essentially forecasting, based on previous time stamp output. The neural network is trained with different layers as shown in Table 6. It is clear from the table that the neural network trained with 11 hidden layers provides the finest R value (percentage of closeness) among others. This justifies the consideration of a proposed 11-layer based feed-forward back-propagation deep neural network-based architecture. This comprises an input layer, 11 hidden layers, and an output layer. The input layer possesses 3x12 neurons, hidden layers hold 12x12 neurons, and the output layer holds 1 neuron as shown in Figure 17. The neurons in the hidden layers are processed through hyperbolic tangential activation function achieving normalized outputs while the output neuron is processed through a linear activation function. The data is split into a ratio of 70:15:15 for training: validation: test. The value of R for the training, validation and testing are 0.9611, 0.9567 and 0.9638 respectively. The overall with Mean Squared Error

Table 6. R-value at different number of hidden layers

Varying Hidden layers-based ANN models	R-value
1	0.9475
2	0.9507
4	0.9517
7	0.9435
10	0.9525
11	0.9603
12	0.9512
14	0.9546

closeness between the observed and the modelled outcome as represented in Figure 22, is quantified with the value of R as tabulated in Table 6. It is clear from Table 6 that the R for the proposed deep-learning based model for the trained locations is closer to unity, reflecting higher prediction capability. Furthermore, the closeness of the deep-learning model with the actual output is reflected in Figure 20 and 21 respectively where the predicted outcome lies in line with the actual value. The value of R is higher for deep-learning based model which involves successive training of weights.

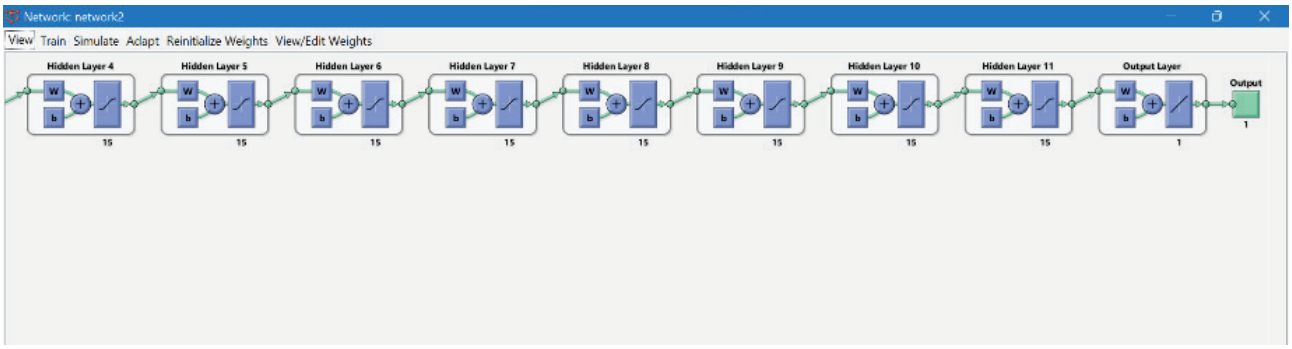

Figure 16. ANN trained on MATLAB.

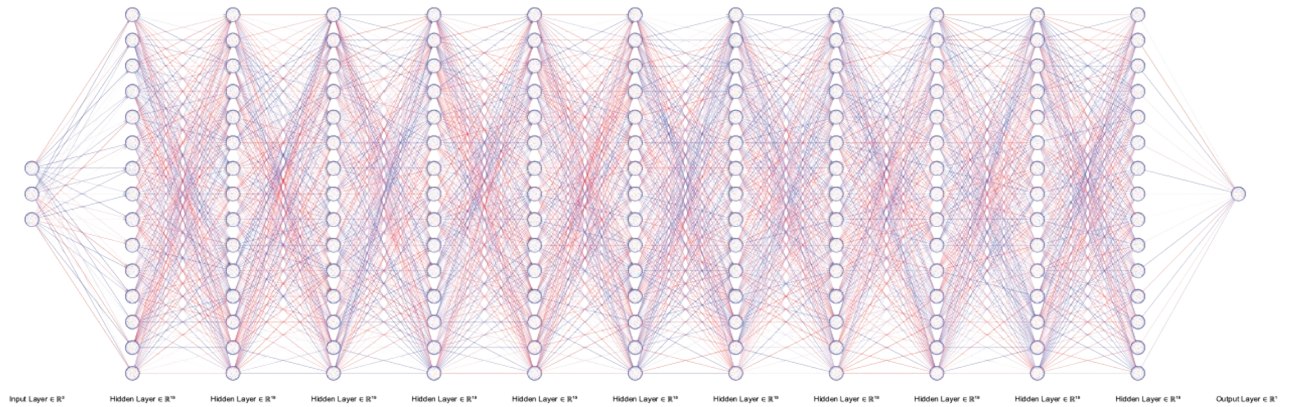

Figure 17. ANN used for model formulation having 11 hidden layers, 1 input layer, and one output layer.

(MSE) is as least as 0.003. Figure 18 shows the comparison of normalized energy generation against the actual as obtained through ANN model for training locations. The error for the proposed ANN model lies between the range of +0.19 to -0.18 as inferred from Figure 19.

An overall comparison among the four proposed models is represented in Figure 20 whose subplot for respective location is shown in Figure 21. The degree of

RESULTS AND DISCUSSION

The process of evaluation of model parameters during validation occurs for two conditions

1. Application of the proposed model for non-trained locations where ground assessment stations exist.
2. Employing the proposed energy estimation models for 380 kW_p PV plant at Bengaluru.

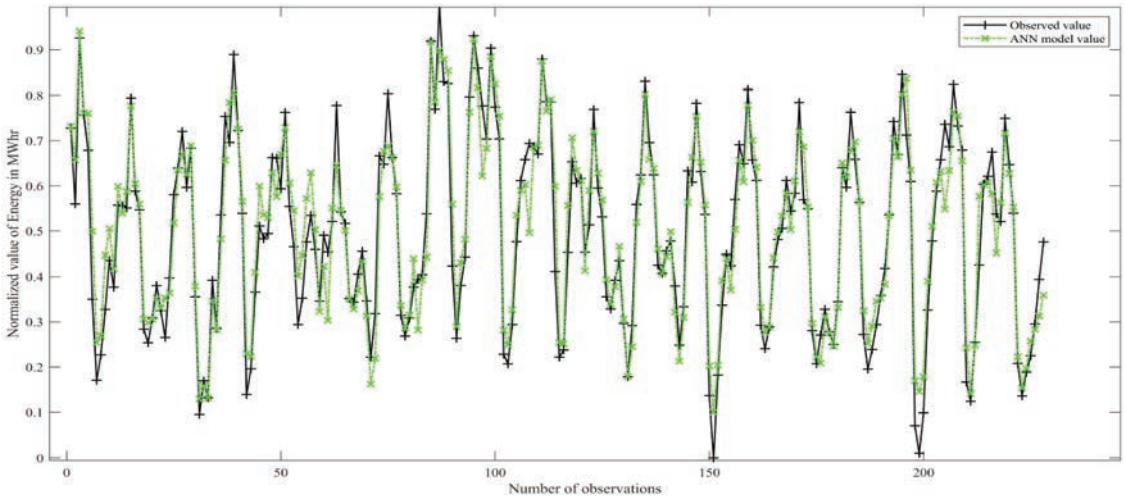

Figure 18. Variation of predicted output employing deep-learning based neural network model with the actual input for energy generated at 19 training locations with errors.

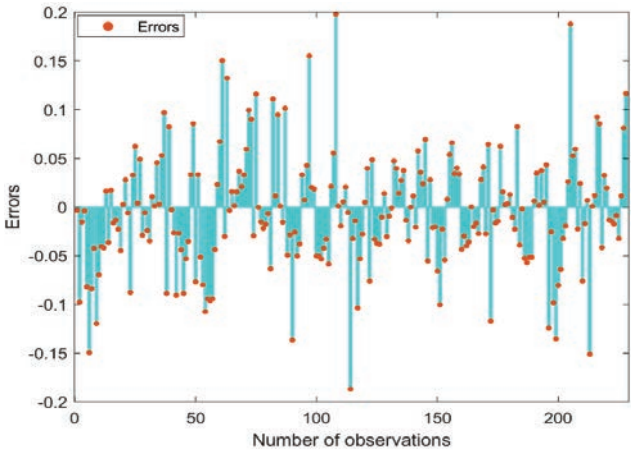

Figure 19. Error in values of calculated energy against the observed value.

The applicability of the formulated model is justified on validation of the proposed model for non-trained locations. The proposed models as in equation (9)-(11) and the deep-learning based ANN are validated for 15 non-trained locations with global irradiance, wind speed and module temperature. It is to highlight that the model co-efficient of the proposed models remains unchanged during the validation process.

A new data set for non-trained locations of 15 in number encompassing ground monitoring and satellite-based stations from RETSCREEN were considered. The overall comparison is shown in Table 7. The overall R for the validation set was found to be 0.9324, 0.8649, 0.9249 and 0.9274 for the linear model, exponential model, non-linear model, and ANN model respectively. The value of R of 0.9274 is reflected through Figure 23 which shows the comparison between the target /actual value and the predicted

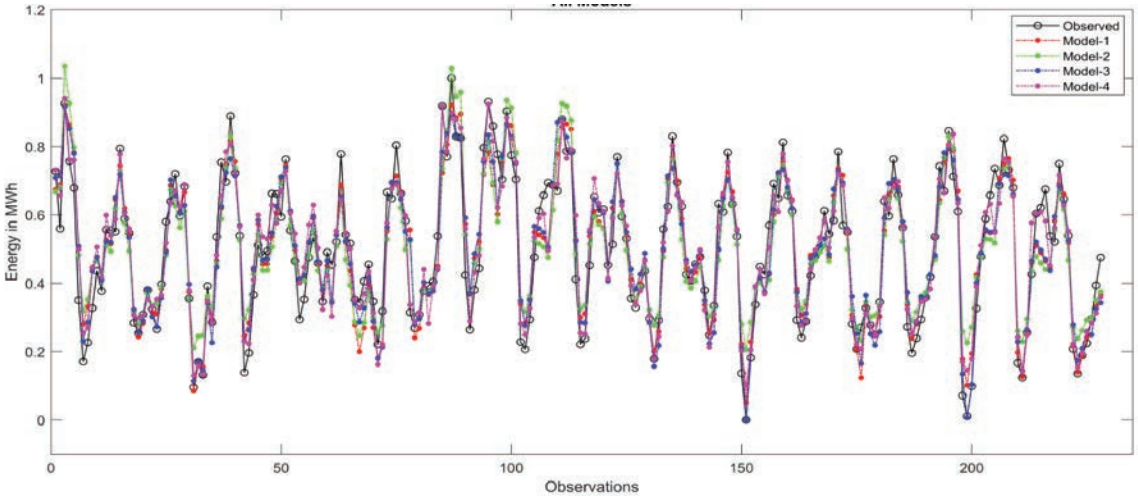

Figure 20. Comparison between all the proposed models with the actual training dataset.

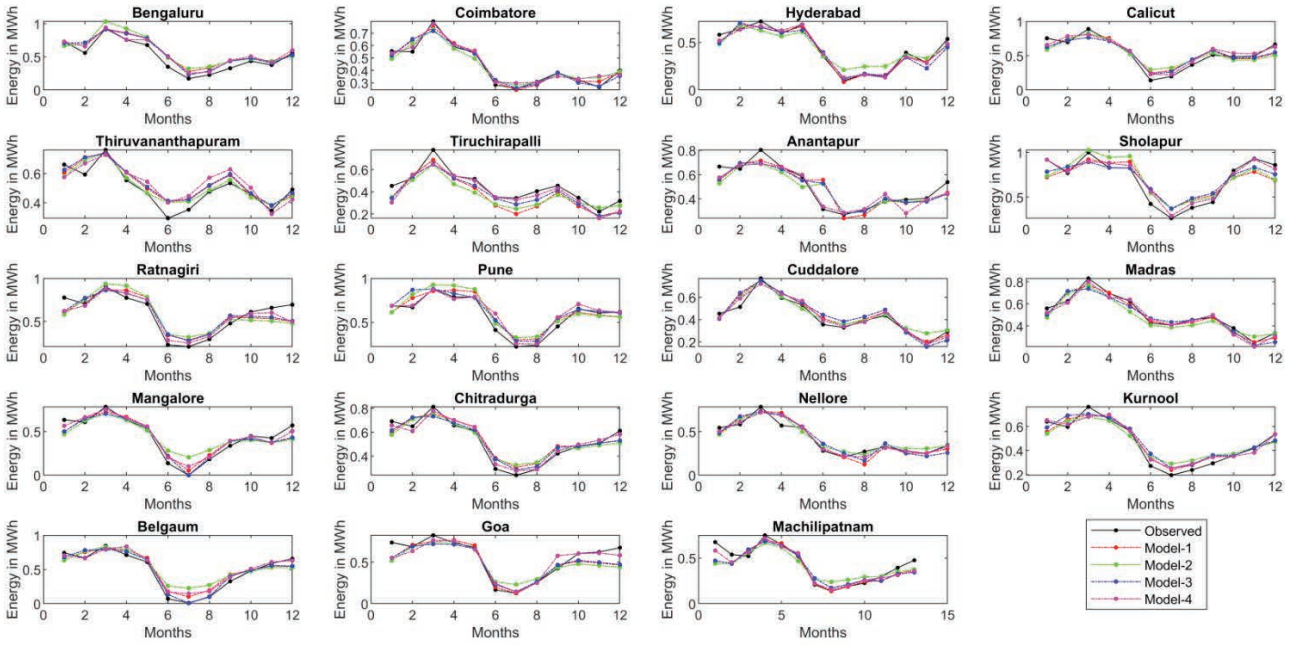

Figure 21. Subplot for training data set considering all models.

Table 7. Value of R for all the models against the training set

Location	R (Linear)	R (Exponential)	R (Non-linear)	R (ANN)
Bangalore	0.9035	0.8684	0.9198	0.9390
Coimbatore	0.9710	0.9619	0.9644	0.9765
Hyderabad	0.9802	0.9367	0.9675	0.9872
Calicut	0.9308	0.8971	0.9321	0.9553
Thiruvananthapuram	0.8811	0.9028	0.8720	0.8089
Tiruchirappalli	0.7691	0.7803	0.8592	0.8630
Anantapur	0.8499	0.8456	0.8679	0.9244
Sholapur	0.8789	0.8837	0.9126	0.9709
Ratnagiri	0.8781	0.8296	0.8954	0.9277
Pune	0.9311	0.9010	0.9254	0.9463
Cuddalore	0.9595	0.9577	0.9238	0.9685
Madras	0.9657	0.9401	0.9410	0.9816
Mangalore	0.9443	0.8769	0.9508	0.9711
Chitradurga	0.9350	0.9283	0.9475	0.9836
Nellore	0.9157	0.9420	0.9126	0.9650
Kurnool	0.9592	0.9331	0.9499	0.9721
Belgaum	0.9550	0.9028	0.9749	0.9664
Goa	0.9049	0.8504	0.9040	0.9342
Machilipatnam	0.9444	0.9066	0.9341	0.9638

energy (response). Higher value of R implies the agreement of closeness between the estimated and the predicted value. The robustness of the proposed model is also justified through higher value of R rendered also during validation. Though linear model possesses similar degree of closeness as deep-learning based ANN, the neural network model meets the uncertainties by successively changing the value of weights and biases for training cycles or epochs yielding

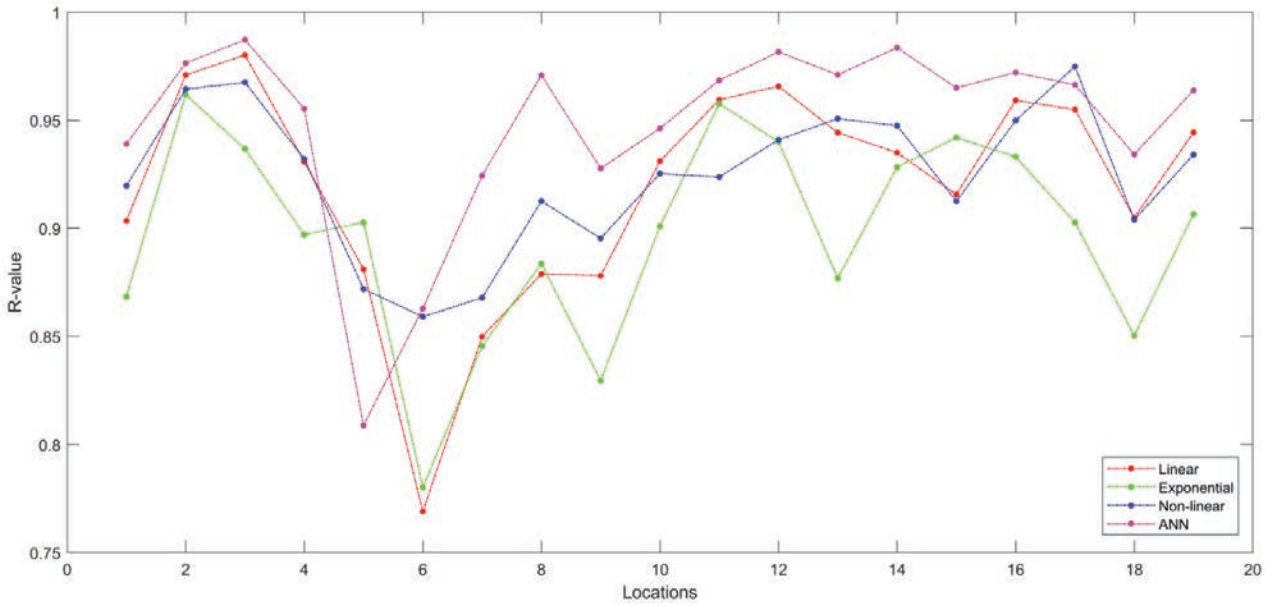

Figure 22. Value of R^2 for all the considered models during training.

Table 8. Validation results for proposed models at additional locations

Location	R (Linear)	R (Exponential)	R (Non-linear)	R (ANN)
Mysore	0.9234	0.8482	0.8783	0.8547
Vellore	0.9330	0.9346	0.8928	0.8946
Warangal	0.9578	0.9329	0.9605	0.9561
Madurai	0.8942	0.9526	0.8581	0.5843
Satara	0.9484	0.9187	0.9629	0.9419
Kolar	0.9113	0.8547	0.8980	0.9276
Selam	0.9092	0.8927	0.8540	0.8177
Vijayawada	0.9440	0.9409	0.9276	0.9617
Nalgonda	0.9490	0.9386	0.9473	0.9590
Gulbarga	0.9097	0.9002	0.9191	0.9497
Bajipur	0.9013	0.8962	0.9191	0.9286
Karwar	0.9258	0.7072	0.8915	0.9281
Kolhapur	0.9423	0.8974	0.9556	0.9423
Udipi	0.9111	0.5556	0.9163	0.9418
Tumakuru	0.9027	0.8032	0.8971	0.9422

better accuracy as seen in Figure 24. The comparison among the estimated and the actual energy generation for all the 15 non-trained locations is represented in Figure 25. The comparison among the estimated and actual energy for the proposed models for all the locations are represented as parity plots in Figure 26 (a)-(d).

The second set of validation has also been carried out from realistic testing inputs acquired from the operational data pertaining to 380 kWp at NMIT, Bengaluru, whose performance analysis is as reported above. A comparison of the proposed models with benchmark models like PVWATTS is also attempted. As seen in Table 9, the proposed model, Model-1, holds good and delivers R, MAE and RMSE of 0.8370, 0.1715, and 0.1389 respectively during validation proving its applicability. A bar plot of actual irradiance and estimated energy for all the locations is illustrated in Figure 27. The minimum value of GHI is seen at 426 W/m^2 corresponding to minimum energy generation,

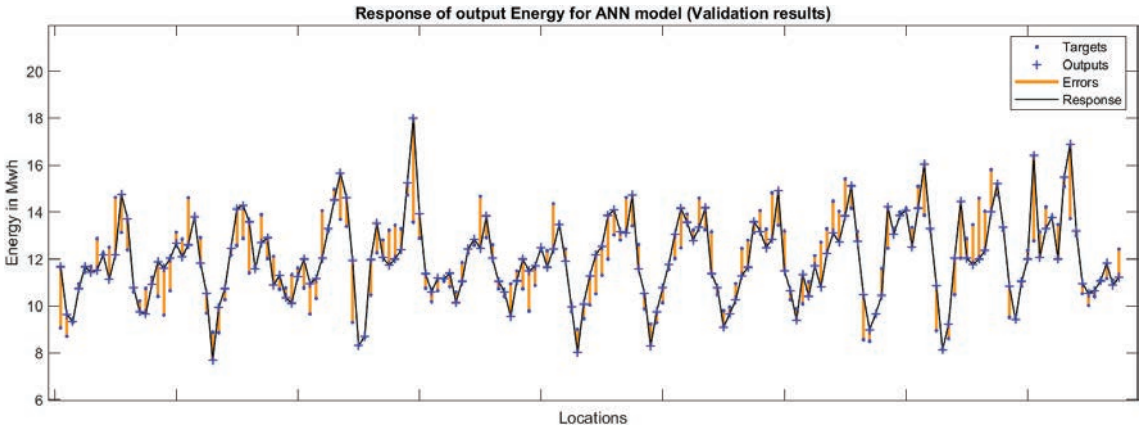

Figure 23. Validation results for proposed deep-learning based neural network model for 15 non-trained locations.

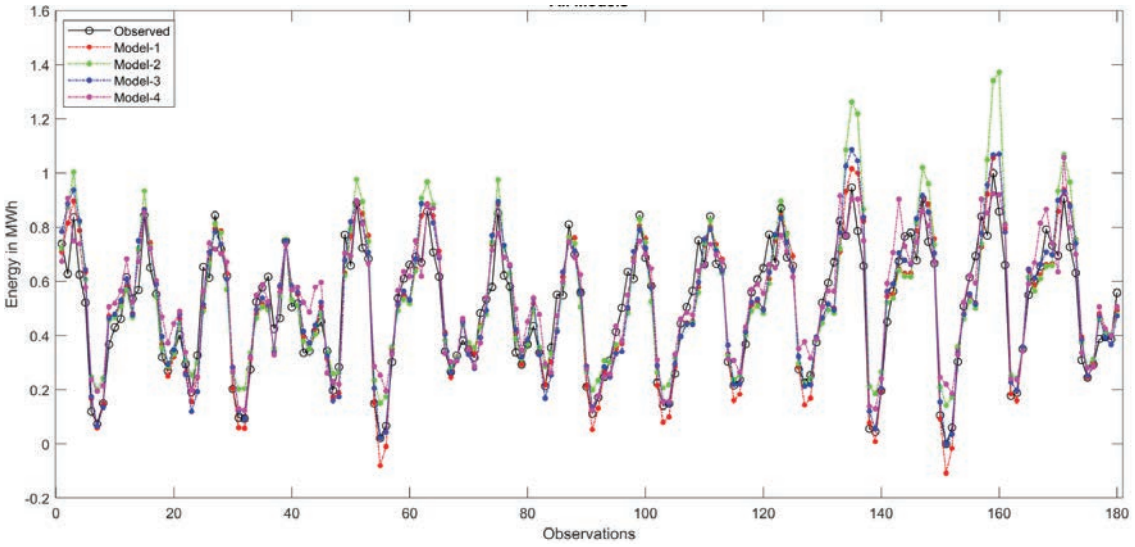

Figure 24. Comparison of test data set with observed values for all the proposed models for 15 non-trained locations.

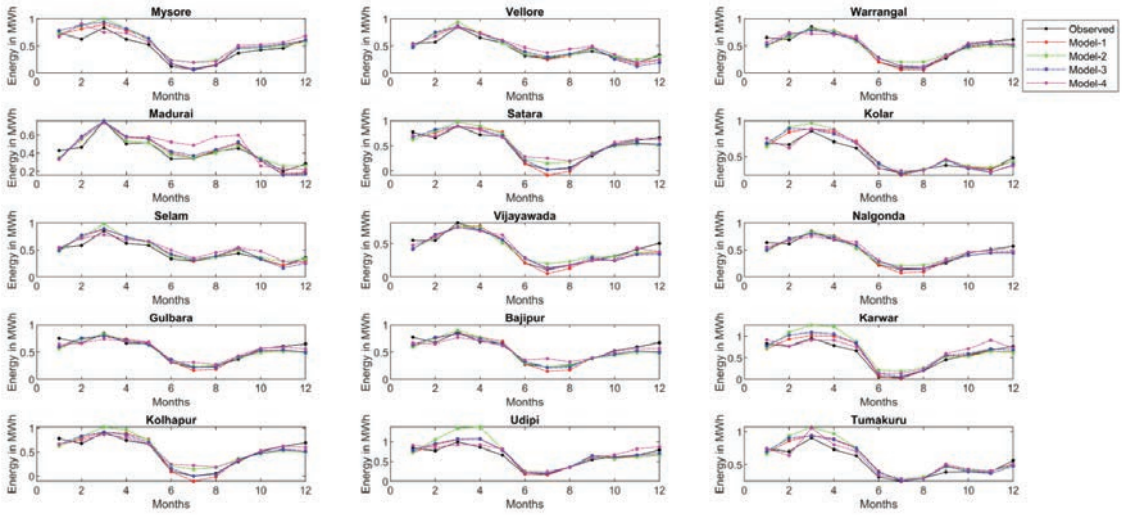

Figure 25. Subplot for test data considering all the proposed models for 15 non-trained locations.

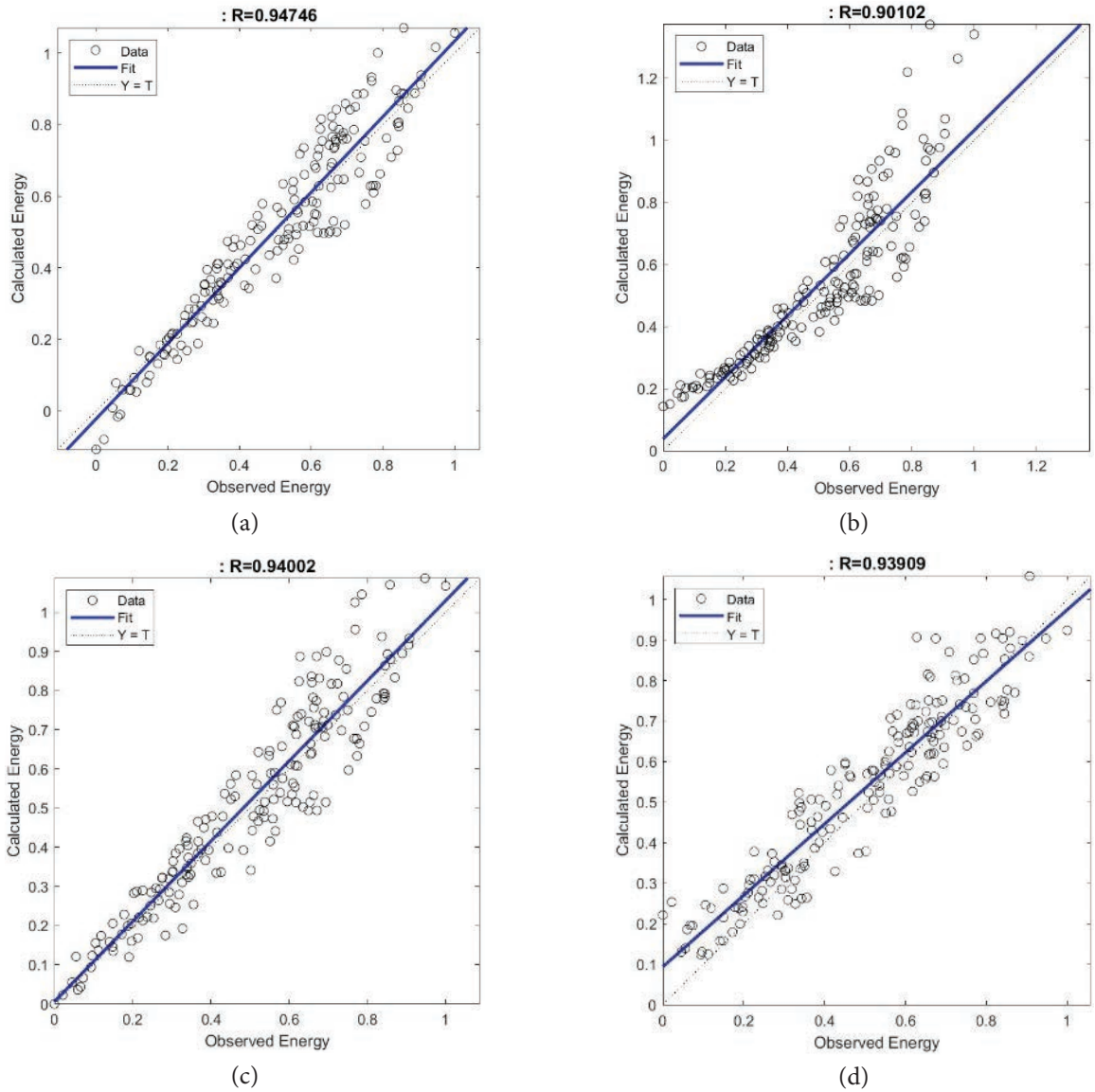

Figure 26. The parity plots for locations stated in Table 8 for (a) Linear, (b) Exponential, (c) Non-Linear, and (d) ANN models.

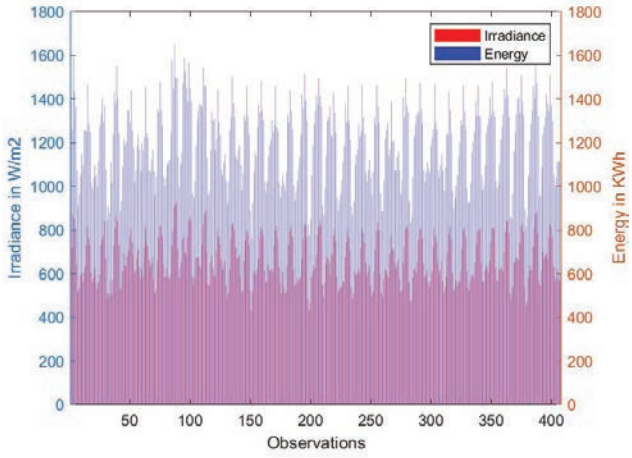

Figure 27. Irradiance and energy generated bar plot for all the considered locations in this study.

while the maximum value of GHI of 930 W/m^2 resulted in maximum energy generation as indicated.

The fitness parameters of the proposed and PVWATSS models like R- value, RMSE and MAE rendered during validation for 380kWp PV plant is graphically illustrated in Figure 28. This clearly justifies the prominence and accuracy of the proposed linear model in comparison with PVWATTS. Validation of the proposed model is also performed against the benchmark PVWATTS calculator whose estimations among the actual is as seen in Figure 29. The proposed model estimates better than the commonly utilized benchmark software PVWATSS where the RMSE and MAE is as least as 0.1715 and 0.1389 respectively. The operational performance of the proposed models varies with respect to locations.

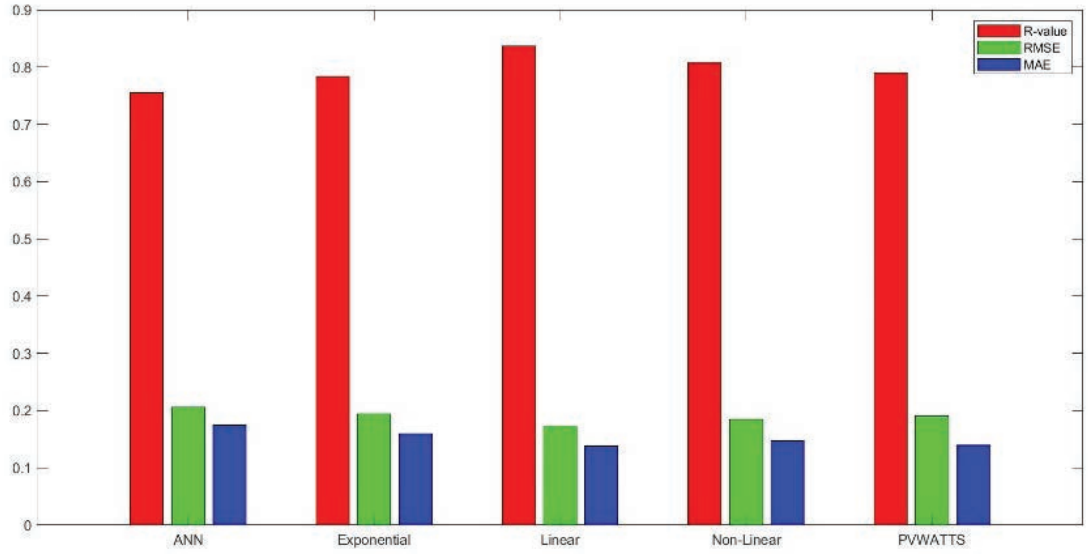

Figure 28. Error based performance parameters during validation for the proposed and the PVWATT model.

Table 9. Validation results in comparison with real-time data and its benchmark against PVWATTS

Validation Benchmark	Model	R	RMSE	MAE
NMIT 380kWp PV	Linear model	0.8370	0.1715	0.1389
	Exponential model	0.7836	0.1946	0.1599
	Non-linear model	0.8077	0.1847	0.1477
	ANN	0.7551	0.2054	0.1746
	PVWATTS	0.79	0.1907	0.1396

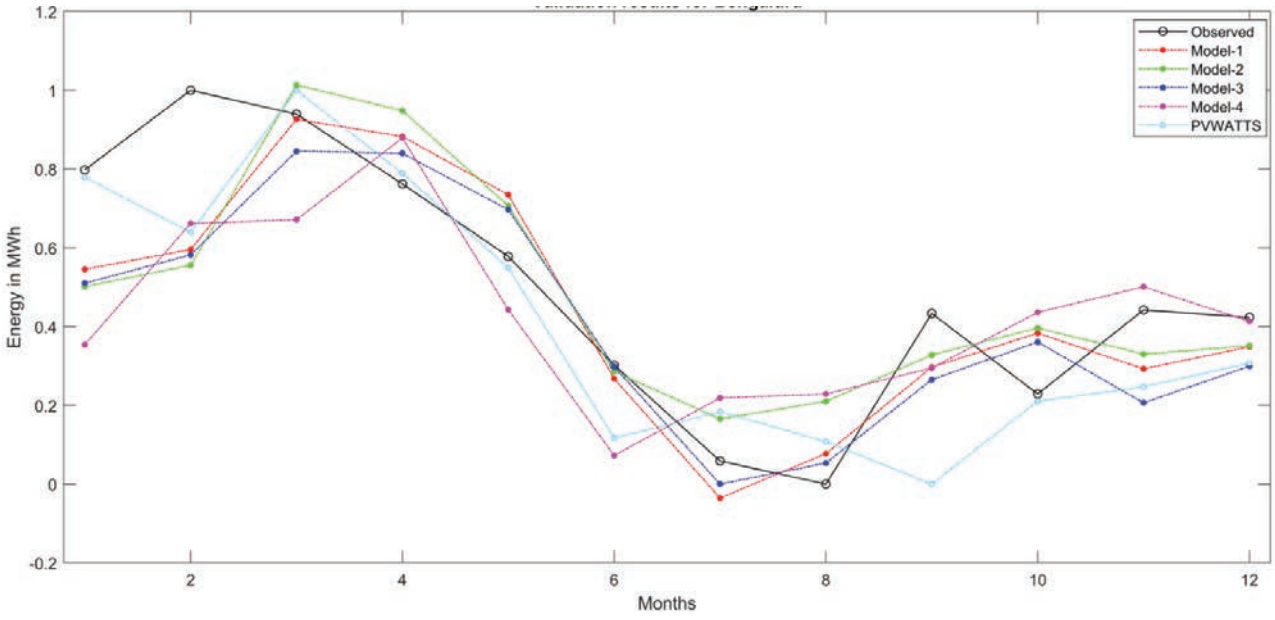

Figure 29. Comparative analysis for validation against PVWATTS for all proposed models for location of Bengaluru from NMIT data.

CONCLUSION

A performance analysis for an annual monitored duration of 2021 -22 is performed for a 380 kWp grid connected PV system. Exergy analysis is also carried out where the annual average exergy efficiency is evaluated as 1.83%. The capacity factor and performance ratio for the plant under investigation are 8.03% and 37% respectively. The reduced performance ratio is due to the fact of least exergy efficiency of the system quantified to 1.83%. This indicates emission of heat during power generation quantified by annual thermal capture losses of 0.46 (h/day). The performance loss rate can also be attributed due to the degradation-based failure modes occurring in the system.

Secondly, the parameters obtained from performance analysis are employed as training and testing data sets for proposed energy prediction models. Models like linear, non-linear and deep learning neural network-based models applicable for locations of South India are proposed as against a model for a location. The deliverable of the proposed model is to estimate energy generation from a distributed generator if the energy meter fails to perform. The models considered in this study are validated for 15 different non-trained locations with varying latitudinal angles ranging from 8.5° to 18.5°. The proposed models are also benchmarked against PVWATTS which is a widely accepted design tool.

The distinct performance-based advantages of the proposed models include

1. All of the proposed models have an R value ranging from 0.75 to 0.84 during validation with no change in model co-efficients for non-trained locations.
2. The proposed linear model (Model-1) gives better performance with an R value of 0.8370 as compared to PVWATTS with an R value of 0.79 for the current location of Bengaluru.

Though the proposed models are trained with a simulation database, the validation of the model is limitedly carried out at two conditions including a realistic plant. The proposed models can thus serve as a realistic pre-estimator-based design tool for Solar Engineers and Solar Entrepreneurs. This will promote the Installation of renewable energy sources leading towards sustainable development.

Through performance analysis of the 380.2 kW_p solar PV system, it is clear that the plant is working nowhere near its maximum capability. A visual inspection was done for all the panels at the site location, and it revealed that the module as well as the system efficiency was so low due to following reasons.

1. Poor to no maintenance for a longer duration has led to accumulation of dust on the glass cover of the panels, leading to soiling losses.
2. Snail trails were found in many panels.
3. Cracks were found in few panels due to mishandling of equipment.
4. Discoloration and hot spots were found in several panels.

These inferences create a scope in near future for accurate quantification of failure effects in commercial Solar PV systems.

NOMENCLATURE

PR	Performance Ratio
Y_f	Final yield (h/day)
Y_r	Referenece yield(h/day)
η_{inv}	Inverter efficiency (%)
η_{sys}	System efficiency (%)
E_{ac}	AC energy generated (kWh/day)
η_{pv}	PV module efficiency
T_m	Module temperature (°C)
T_a	Ambient temperature (°C)
T_s	Suns temperature (K)
w	Wind speed (m/s)
CUF	Capacity Utilization Factor
H	Solar irradiance(kWh/m^2/day)

ACKNOWLEDGEMENT

The authors wish to thank Nitte Meenakshi Institute of Technology for providing access for 380.2 kWp solar PV power plant and acknowledge their contribution in fulfilment of this study.

AUTHORSHIP CONTRIBUTIONS

Authors equally contributed to this work.

DATA AVAILABILITY STATEMENT

The authors confirm that the data that supports the findings of this study are available within the article. Raw data that support the finding of this study are available from the corresponding author, upon reasonable request.

CONFLICT OF INTEREST

The author declared no potential conflicts of interest with respect to the research, authorship, and/or publication of this article.

ETHICS

There are no ethical issues with the publication of this manuscript.

REFERENCES

[1] IEA. India energy policy review 2020. Available at: https://niti.gov.in/sites/default/files/2020-01/IEA-India 2020-In-depth-EnergyPolicy_0.pdf. Accessed Aug 7, 2024.

[2] BP. Statistical review of world energy 2021. Available at: https://www.bp.com/content/dam/bp/business-sites/en/global/corporate/pdfs/energy-economics/statistical-review/bp-stats-review-2021-full-report.pdf. Accessed Aug 7, 2024.
[3] Uyan M. GIS-based solar farms site selection using analytic hierarchy process (AHP) in Karapinar region, Konya/Turkey. Renew Sustain Energy Rev 2013;28:11-17. [CrossRef]
[4] Kaiser P, Unde RB, Kern C, Jess A. Production of liquid hydrocarbons with CO2 as carbon source based on reverse water-gas shift and Fischer-Tropsch synthesis. Chem Ing Tech 2013;85:489-499. [CrossRef]
[5] Ali S, Taweekun J, Techato K, Waewsak J, Gyawali S. GIS based site suitability assessment for wind and solar farms in Songkhla, Thailand. Renew Energy 2019;132:1360-1372. [CrossRef]
[6] Noorollahi Y, Yousefi H, Mohammadi M. Multi-criteria decision support system for wind farm site selection using GIS. Sustain Energy Technol Assess 2016;13:38-50. [CrossRef]
[7] Aydin NY, Kentel E, Sebnem Duzgun H. GIS-based site selection methodology for hybrid renewable energy systems: A case study from western Turkey. Energy Conver Manage 2013;70:90-106. [CrossRef]
[8] Heras-Saizarbitoria I, Cilleruelo E, Zamanillo I. Public acceptance of renewables and the media: An analysis of the Spanish PV solar experience. Renew Sustain Energy Rev 2011;15:4685-4696. [CrossRef]
[9] Tabassum A, Premalatha M, Abbasi T, Abbasi SA. Wind energy: Increasing deployment, rising environmental concerns. Renew Sustain Energy Rev 2014;31:270-288. [CrossRef]
[10] Ministry of Renewable Energy, India. Solar - Current Status. Available at: www.mnre.gov.in/solar/current-status. Accessed Dec 23, 2021.
[11] IEA; International Renewable Energy Agency; United Nations Statistics Division; The World Bank; World Health Organization. Tracking SDG 7: The energy progress report - 2019. Available at: https://www.irena.org/-/media/Files/IRENA/Agency/Publication/2019/May/2019-Tracking-SDG7-Report.pdf?rev=30fdda95ad074b6eb27c8aa4347605e8. Accessed Aug 7, 2024.
[12] Huang Q, Wei S. Improved quantile convolutional neural network with two-stage training for daily-ahead probabilistic forecasting of photovoltaic power. Energy Conver Manage 2020;220:113085. [CrossRef]
[13] Meng X, Gao F, Xu T, Zhou K, Wei L, Wu Q. Inverter-data-driven second-level power forecasting for photovoltaic power plant. IEEE Trans Ind Electron 2020;68:7034-7044. [CrossRef]
[14] Yan J, Hu L, Zhen Z, Qiu G, Li Y, Yao L, et al. Frequency-domain decomposition and deep learning based solar PV power ultra-short-term forecasting model. IEEE Trans Ind Appl 2021;57:3282-32-92. [CrossRef]
[15] Ahmed R, Sreeram V, Mishra Y, Arif MD. A review and evaluation of the state-of-the-art in PV solar power forecasting: Techniques and optimization. Renew Sustain Energy Rev 2020;124:109792. [CrossRef]
[16] Mellit A, Kalogirou SA. Artificial intelligence techniques for photovoltaic applications: A review. Prog Energy Combust Sci 2008;34:574-632. [CrossRef]
[17] Bhowmik M, Naik BK, Muthukumar P, Anandalakshmi R. Performance assessment and optimization of liquid desiccant dehumidifier system using intelligent models and integration with solar dryer. J Build Engineer 2023;64:105577. [CrossRef]
[18] Bhowmik M, Muthukumar P, Anandalakshmi R. Experimental based multilayer perceptron approach for prediction of evacuated solar collector performance in humid subtropical regions. Renew Energy 2019;143:1566-1580. [CrossRef]
[19] Baharin KA, Rahman HA, Hassan MY, Gan CK. Short-term forecasting of solar photovoltaic output power for tropical climate using ground-based measurement data. J Renew Sustain Energy 2016;8:053701. [CrossRef]
[20] Kim YS, Joo HY, Kim JW, Jeong SY, Moon JH. Use of a big data analysis in regression of solar power generation on meteorological variables for a Korean solar power plant. Appl Sci 2021;11:1776. [CrossRef]
[21] Sheng H, Xiao J, Cheng Y, Ni Q, Wang S. Short-term solar power forecasting based on weighted gaussian process regression. IEEE Trans Ind Electron 2018;65:300-308. [CrossRef]
[22] Smithson SC, Yang G, Gross WJ, Meyer BH. Neural networks designing neural networks: Multi-objective hyper-parameter optimization. IEEE/ACM International Conference on Computer - Aided Design; 2016. pp. 1-8. [CrossRef]
[23] Sundaram S, Babu JSC. Performance evaluation and validation of 5 MWp grid connected solar photovoltaic plant in South India. Energy Conver Manage 2015;100:429-439. [CrossRef]
[24] Yadav SK, Bajpai U. Performance evaluation of a rooftop solar photovoltaic power plant in Northern India. Energy Sustain Dev 2018;43:130-138. [CrossRef]
[25] Kymakis E, Kalykakis S, Papazoglou TM. Performance analysis of a grid connected photovoltaic park on the island of Crete. Energy Conver Manage 2009;50:433-438. [CrossRef]
[26] Ayompe LM, Duffy A, McCormack SJ, Conlon M. Measured performance of a 1.72 kW rooftop grid connected photovoltaic system in Ireland. Energy Conver Manage 2011;52:816-825. [CrossRef]
[27] Kumar M, Kumar A. Performance assessment and degradation analysis of solar photovoltaic technologies: A review. Renew Sustain Energy Rev 2017;78:554-587. [CrossRef]
[28] Saitoh H, Hamada Y, Kubota H, Nakamura M, Ochifuji K, Yokoyama S, et al. Field experiments

and analyses on a hybrid solar collector. Appl Therm Engineer 2003;23:2089-2105. [CrossRef]

[29] Sundaram S. Performance assessment with the prediction of final yield and performance ratio employing artificial neural network for a realistic 1 MWp PV plant in India. Int J Ambient Energy 2022;43:1739-1750. [CrossRef]

[30] Kumar BS, Sudhakar K. Performance evaluation of 10 MW grid connected solar photovoltaic power plant in India. Energy Rep 2015;1:184-192. [CrossRef]

[31] Padmavathi K, Daniel SA. Performance analysis of a 3 MWp grid connected solar photovoltaic power plant in India. Energy Sustain Dev 2013;17:615-625. [CrossRef]